

Acoustic Localization of Transient Signals with Wind Compensation

by Brandon Au, Ananth Sridhar, and Geoffrey Goldman

ARL-TR-6318

January 2013

NOTICES

Disclaimers

The findings in this report are not to be construed as an official Department of the Army position unless so designated by other authorized documents.

Citation of manufacturer's or trade names does not constitute an official endorsement or approval of the use thereof.

Destroy this report when it is no longer needed. Do not return it to the originator.

Army Research Laboratory

Adelphi, MD 20783-1197

ARL-TR-6318**January 2013**

Acoustic Localization of Transient Signals with Wind Compensation

Brandon Au, Ananth Sridhar, and Geoffrey Goldman
Sensors and Electron Devices Directorate, ARL

REPORT DOCUMENTATION PAGE				Form Approved OMB No. 0704-0188	
<p>Public reporting burden for this collection of information is estimated to average 1 hour per response, including the time for reviewing instructions, searching existing data sources, gathering and maintaining the data needed, and completing and reviewing the collection information. Send comments regarding this burden estimate or any other aspect of this collection of information, including suggestions for reducing the burden, to Department of Defense, Washington Headquarters Services, Directorate for Information Operations and Reports (0704-0188), 1215 Jefferson Davis Highway, Suite 1204, Arlington, VA 22202-4302. Respondents should be aware that notwithstanding any other provision of law, no person shall be subject to any penalty for failing to comply with a collection of information if it does not display a currently valid OMB control number.</p> <p>PLEASE DO NOT RETURN YOUR FORM TO THE ABOVE ADDRESS.</p>					
1. REPORT DATE (DD-MM-YYYY) January 2013		2. REPORT TYPE Final		3. DATES COVERED (From - To)	
4. TITLE AND SUBTITLE Acoustic Localization of Transient Signals with Wind Compensation				5a. CONTRACT NUMBER	
				5b. GRANT NUMBER	
				5c. PROGRAM ELEMENT NUMBER	
6. AUTHOR(S) Brandon Au, Ananth Sridhar, and Geoffrey Goldman				5d. PROJECT NUMBER	
				5e. TASK NUMBER	
				5f. WORK UNIT NUMBER	
7. PERFORMING ORGANIZATION NAME(S) AND ADDRESS(ES) U.S. Army Research Laboratory ATTN: RDRL-SES-P 2800 Powder Mill Road Adelphi, MD 20783-1197				8. PERFORMING ORGANIZATION REPORT NUMBER ARL-TR-6318	
9. SPONSORING/MONITORING AGENCY NAME(S) AND ADDRESS(ES)				10. SPONSOR/MONITOR'S ACRONYM(S)	
				11. SPONSOR/MONITOR'S REPORT NUMBER(S)	
12. DISTRIBUTION/AVAILABILITY STATEMENT Approved for public release; distribution unlimited.					
13. SUPPLEMENTARY NOTES					
14. ABSTRACT <p>Accurate target localization of hostile weapons fire is an area of interest for the U.S. Army. While visual cues may provide a point of origin of weapon's fire, the acoustic signal of the shot can give a more accurate estimate. Using multiple microphone arrays, the position of a source can be estimated by using estimated times of arrival (TOAs) and angles of arrival (AOAs) computed at each array. However, noise from other sources reduces the accuracy of the algorithms. Wind reduces localization accuracy by adding bias to the AOA and TOA estimates. In some instances, wind data are not collected. Blind wind estimation can still be used to adjust localization results. The goal of this work is to take impulsive acoustic data collected with four microphone arrays and estimate the location of the source with an algorithm that accounts for the effect of wind. The model uses constant wind speed. The source location is estimated using least squares and maximum likelihood algorithms. The results indicate that there are improvements in localization accuracy using algorithms processed with meteorological data and blind wind estimation techniques.</p>					
15. SUBJECT TERMS Localization acoustic wind					
16. SECURITY CLASSIFICATION OF:			17. LIMITATION OF ABSTRACT UU	18. NUMBER OF PAGES 28	19a. NAME OF RESPONSIBLE PERSON Geoffrey Goldman
a. REPORT Unclassified	b. ABSTRACT Unclassified	c. THIS PAGE Unclassified			19b. TELEPHONE NUMBER (Include area code) (301) 394-0882

Contents

List of Figures	iv
List of Tables	iv
Acknowledgments	v
1. Introduction	1
2. Experiment/Calculations	1
3. Results and Discussion	5
3.1 No Wind Compensation	5
3.2 Estimation with Meteorological Data.....	7
3.3 Estimation Using Blind Wind Compensation	8
3.4 Comparative Performance	11
4. Conclusions	17
5. References	18
List of Symbols, Abbreviations, and Acronyms	19
Distribution List	20

List of Figures

Figure 1. Location of sensor arrays. The source is at the origin.	2
Figure 2. Geometry for localizing a source using DOA.	3
Figure 3. Blind wind estimates day 9.....	10
Figure 4. Blind wind estimates day 10.....	11
Figure 5. Estimated position error using AOA data only on day 9.....	13
Figure 6. Estimated position error using TOA data only on day 9.	13
Figure 7. Estimated position error using both AOA and TOA data on day 9.....	14
Figure 8. Estimated position error using AOA data only on day 10.....	14
Figure 9. Estimated position error using TOA data only on day 10.	15
Figure 10. Estimated position error using both AOA and TOA data on day 10.....	15

List of Tables

Table 1. Source position errors on day 9 using MLE with no wind compensation.	6
Table 2. Source position errors on day 10 using MLE with no wind compensation.	7
Table 3. Source position errors on day 9 using MLE with met data.	8
Table 4. Source position errors on day 10 using MLE with met data.	8
Table 5. Source estimates' errors with blind wind estimation for day 9.	9
Table 6. Source estimates' errors with blind wind estimation for day 10.	10
Table 7. Results for day 9 without wind compensation.....	11
Table 8. Results for day 9 with meteorological wind data.	11
Table 9. Results for day 9 with blind wind estimation.	12
Table 10. Results for day 10 without wind compensation.....	12
Table 11. Results for day 10 using meteorological wind data.	12
Table 12. Data error metrics for day 10 with blind wind estimation.....	12
Table 13. Percent reduction in distance error over no wind estimate.....	12

Acknowledgments

We wish to thank Kirk Alberts and Leng Sim for their support and contributions.

INTENTIONALLY LEFT BLANK.

1. Introduction

The U.S. Army Research Laboratory is interested in detecting and tracking targets with high accuracy, low cost, and low power (1–4). Multiple microphone arrays are commonly employed as alternatives to radar and other sensors. Using results collected by multiple microphone arrays, localization algorithms are able to triangulate the location of an acoustic source (5, 6). The collected data included the time of arrival (TOA) and angles of arrival (AOAs) of detected signals. Using these data sets, we can implement least squares and maximum likelihood algorithms to estimate the source position. One common cause of localization error is wind noise. Wind alters the path sound will travel between the source and the microphone array, thus altering TOA and AOA. While the effect may be small, compensating for wind should improve localization accuracy. When wind data are not collected, blind wind estimation methods can be used.

Two approaches were developed to compensate for the effects of wind. A least squares estimated position could be found using geometry and minimizing the cost function of the dot product of the direction of arrival (DOA) and the vector between the array and estimated source location. Also, maximum likelihood estimates of the position were calculated for TOA and DOA estimates corrupted by Gaussian noise. By iteratively calculating the error at each point in a grid around the least squares estimate, a maximum likelihood estimate can be found. Algorithms were tested using data collected at the Blossom Point Research Facility (BPRF) in 2011. Meteorological data were simultaneously collected with the acoustic signals using a wind sensor at a height of approximately 2 m within the footprint of the acoustic arrays.

In this report, we first discuss the algorithms used to compute the least squares and maximum likelihood source estimates without wind, and then the maximum likelihood source estimates using collected meteorological data and blind wind estimation. Then, we discuss our testing and collection of results using data collected from BPRF. Finally, we discuss which method performs the best, along with our observations and conclusions.

2. Experiment/Calculations

Data collected at BPRF were measured using four 1-m tetrahedral microphone arrays over a three-day experimental period. Each array continuously collected data for the entire day. The arrays returned various messages, each containing specific pieces of data depending on the purpose of those messages. For this data, the two types of messages needed were “Heading” (HEDG) and “Line of Bearing” (LOBR). HEDG messages contain global positioning system (GPS) corrections for the array bearing with respect to true north. LOBR messages contain data

from the detections of potential weapon's fire, including AOA, TOA, array GPS position, and noise power. Figure 1 shows the layout of the testing area, with the source located at the origin and Array 4 located closest to the source.

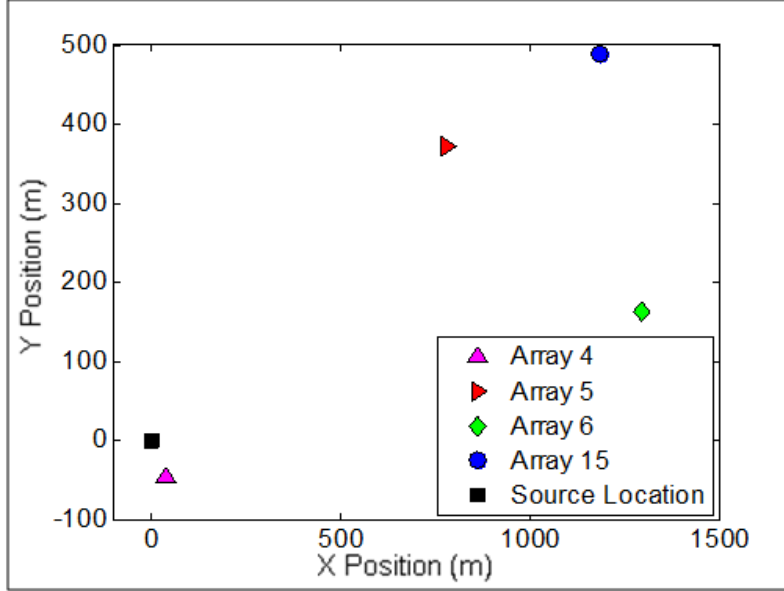


Figure 1. Location of sensor arrays. The source is at the origin.

Before calculating an estimated position of the source, data association is required to match the data collected by all four microphone arrays. The propagation time delay between arrays can be greater than 5 s. First, the AOA estimates within a 45° window on either side of the median AOA of the source were grouped together. A 90° window was chosen because it fit the data and a fixed source should have a window of probable AOA that is large enough to include signals affected by the wind, but not take signals that are coming from implausible directions. The final process uses the TOA data and the time of travel between arrays to associate the data. By choosing the array closest to the source based on the noise power data, the time of travel between that array and the others should be close to the known difference in TOA. Therefore, the detections that agree with the times of travel would indicate the same shot is heard.

After data association, a localization algorithm is implemented for every shot. Figure 2 shows the geometry of the localization problem. The source position is estimated using

$$\left(R_{90}\vec{a}_n\right) \bullet \left(\vec{P}_n - \vec{S}\right) = 0 \quad (1)$$

where R_{90} is a 90° rotation matrix, \vec{a}_n is the DOA of array n , \vec{P}_n is the location of n^{th} array, and \vec{S} is the source position (4).

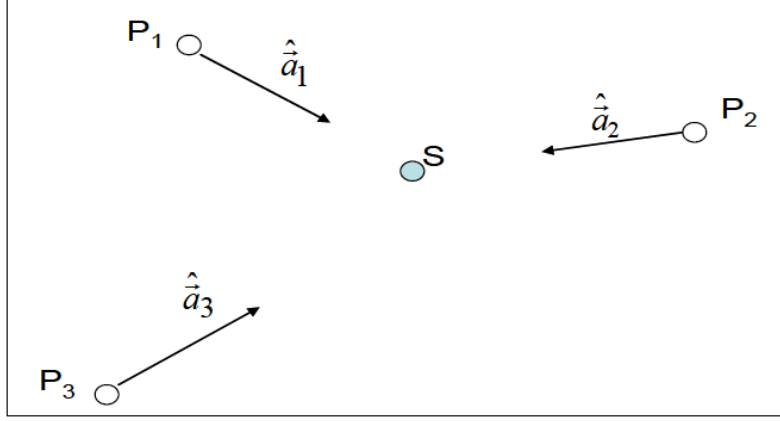


Figure 2. Geometry for localizing a source using DOA.

The solution for source position that minimizes the squared error is

$$\hat{\vec{S}} = \left(A^T C_Y^{-1} A \right)^{-1} A^T C_Y^{-1} Y \quad (2)$$

where

$$Y_m = P_m^T R_{90} \vec{a}_m, \quad (3)$$

$$A = \begin{bmatrix} (R_{90} \vec{a}_1)^T \\ \vdots \\ (R_{90} \vec{a}_M)^T \end{bmatrix}, \quad (4)$$

and

$$C_Y = \begin{bmatrix} \sigma_{Y_1}^2 & 0 & 0 \\ 0 & \ddots & 0 \\ 0 & 0 & \sigma_{Y_M}^2 \end{bmatrix} \quad (5)$$

where $\sigma_{Y_i}^2$ is the DOA variance at each array (4). The variance was chosen as the AOA variance for all shots at each array. Using these equations, a least squares estimate of the source position is obtained for each shot.

TOA can be included in the calculations to improve the accuracy and consistency of the results. To use TOA estimates, a maximum likelihood algorithm was employed to best fit both TOA and AOA using the least squares estimated position as the starting point. By searching for the source position in a 100×100 grid around the estimated position, a maximum likelihood estimate (MLE) of the source position can be found. The MLE is given by

$$L(x_1, x_2, \dots, x_n; \theta) \triangleq \log f_x(x_1, x_2, \dots, x_n; \theta) \quad (6)$$

where $L(x_1, x_2, \dots, x_n; \theta)$ is the likelihood function and $f_x(x_1, x_2, \dots, x_n; \theta)$ is the joint probability density function (8). To simplify the calculations, the measurement noise was assumed to be independent and Gaussian distributed, which reduces the likelihood function to a summation of squared terms. Therefore, to find the maximum likelihood solution, it involved minimizing the squared difference between the collected data and the calculated position data for each shot. For the AOA data, the formula used for each microphone is

$$\text{Cost1} = \sum_{k=1}^n \frac{1}{W_k} (AOA_k - AOA_{k_{calc}})^2 \quad (7)$$

where n is the number of microphone arrays, W_k is weighting term of array k , AOA_k is the collected AOA at array k , and $AOA_{k_{calc}}$ is the calculated AOA found at the current position of the grid search. The weighting terms were taken as two times the variance of the AOA at each array. Because TOA was not collected relative to event start time, differential time of arrival (DTOA) was used.

$$\text{Cost2} = \sum_{i=1}^n \sum_{j=i+1}^n \frac{1}{W_{i,j}} \left((TOA_i - TOA_j) - (TOA_{i_{calc}} - TOA_{j_{calc}}) \right)^2 \quad (8)$$

where n is the number of arrays, $W_{i,j}$ is the weighting term between arrays i and j , TOA_i is the collected TOA for array i , and $TOA_{i_{calc}}$ is the calculated TOA for array i found at the current position of the grid search. The weighting terms were taken again as two times the variance of the difference between the TOA at each array pair. Using these two techniques, a best estimate of the source location can be found by minimizing the sum of cost1 and cost2. This was done for every shot.

These algorithms were modified to compensate for the effect of wind. The propagation delay time is modeled using

$$TOA = \frac{\left\| \vec{S} - (\vec{P} + (\overrightarrow{wind} \times TOA)) \right\|}{c} \quad (9)$$

where \vec{S} is the estimated source position, \vec{P} is the array position, \overrightarrow{wind} is the wind velocity, and c is the speed of sound (340 m/s). The MLE solution can be determined by minimizing the cost function

$$\text{Cost3} = \sum_{i=1}^n \sum_{j=i+1}^n \frac{1}{W_{i,j}} \left((TOA_i - TOA_j) - (TOA_{i_{calc}} - TOA_{j_{calc}}) \right)^2 \quad (10)$$

where n is the number of arrays, $W_{i,j}$ is the weighting term between arrays i and j , and TOA_i is the collected TOA for array i . By searching for the wind velocity and position that minimizes the cost, the position of the source can be estimated.

To improve this search, AOA can also be used after TOA calculations. Simplifying the algorithm again as described above, the AOA algorithm used was

$$\tan \theta = \left(\frac{\vec{S}_y - (\vec{P}_y + \vec{wind}_y \times time)}{\vec{S}_x - (\vec{P}_x + \vec{wind}_x \times time)} \right) \quad (11)$$

where θ is the new AOA found through the grid search and $time$ is calculated from the maximum likelihood algorithm using equation 9. By treating the noise as independent and Gaussian distributed, the maximum likelihood is the square difference of the data and the new calculated θ . By finding the square difference between θ and the array's AOA estimate, then dividing by the variance of the AOA data, the MLE of the source location can be found as shown below

$$Cost4 = \sum_{k=1}^n \frac{1}{W_k} (AOA_k - \theta_k)^2 \quad (12)$$

where n is the number of arrays, AOA_k is the AOA for array k from the processed data, θ_k is calculated from equation 11, and W_k is the weighting term, again chosen as two times to variance of the AOA at array k .

To provide the best result, both TOA and AOA results should be used simultaneously in an algorithm. This is accomplished by adding the two cost functions and finding the minimum:

$$Cost5 = \frac{1}{W_{AOA}} \sum_{k=1}^n \frac{1}{W_k} (AOA_k - AOA_{k_{calc}})^2 + \frac{1}{W_{TOA}} \sum_{i=1}^n \sum_{j=i+1}^n \frac{1}{W_{i,j}} \left((TOA_i - TOA_j) - (TOA_{i_{calc}} - TOA_{j_{calc}}) \right)^2 \quad (13)$$

where $\frac{1}{W_{AOA}}$ is a weighting term for the AOA maximum likelihood and $\frac{1}{W_{TOA}}$ is a weighting term for the TOA maximum likelihood.

3. Results and Discussion

3.1 No Wind Compensation

After initial attempts at data association, the processed data from one array (array 4) were found to be inconsistent due to signal saturation. To resolve this problem, new algorithms were developed to process the raw data from array 4. This involved using different methods of identifying when the signal “arrives” at the array, and determining AOA based on the difference in TOA at each microphone on the array. Using this variety of methods, a best choice was chosen so that the maximum likelihood error was minimized. After testing the new algorithms, one method had 100% detection for the shots measured on array 4. Some outliers were still present, but they were removed in the data association algorithm. However, an offset error between the old and new TOA estimates was created. A user-defined constant must be added to

match the TOA offsets of a given shot for data association. Data association relies on matching the TOAs together. Without this offset, the DTOA between the other arrays and the saturated array would never be close enough. However, this offset makes the TOA invalid for comparing with the other arrays. To remove this, maximum likelihood source estimates were calculated using AOA data from all arrays and/or only the TOA from the non-saturating arrays.

Before wind compensation, a MLE is computed. From equation 2, a least squares estimate was found using only the AOA. Combining equations 7 and 8, a MLE was found. Because TOA for the one array is invalid, MLEs were computed using results from three arrays. Therefore, some estimates did not use every data set available and thus not every equation was used. Using AOA or both AOA and TOA returned similar results for MLE, while using TOA only returned a poorer results. Tables 1 and 2 show the error in the estimated position to the source for every shot detected.

Table 1. Source position errors on day 9 using MLE with no wind compensation.

	Est. from AOA	Est. from TOA	Est. from Both
Shot	Distance (meters)	Distance (meters)	Distance (meters)
1	37.10	114.59	37.10
2	2.45	103.63	2.45
3	3.13	88.83	3.13
4	17.04	103.84	17.04
5	22.41	97.37	22.41
6	19.95	107.81	19.95
7	28.09	110.29	28.09
8	46.44	119.04	46.44
9	3.52	90.63	3.52
10	38.96	118.09	38.96
11	21.82	117.76	21.82
12	5.69	98.03	5.69
13	34.24	125.07	34.24
14	8.39	43.57	8.39
15	37.71	98.76	37.71
16	49.77	56.35	49.77
17	20.00	125.94	20.00
18	21.94	92.73	21.94
19	49.63	137.62	49.63
20	38.19	124.31	38.19
Median	22.18	105.82	22.18
Mean	25.32	103.71	15.70

Table 2. Source position errors on day 10 using MLE with no wind compensation.

	Est. from AOA	Est. from TOA	Est. from Both
Shot	Distance (meters)	Distance (meters)	Distance (meters)
1	17.30	105.97	17.30
2	22.00	110.08	22.00
3	18.45	108.34	18.45
4	9.82	111.57	9.82
5	16.03	148.24	16.03
6	59.70	184.02	59.70
7	33.90	128.35	33.90
8	51.18	116.89	51.18
9	28.61	22.19	28.61
10	29.09	114.04	29.09
Median	25.30	112.81	25.30
Mean	28.61	114.97	28.61

3.2 Estimation with Meteorological Data

To improve of these estimates, algorithms were developed to compensation for wind effects. First, the position of the source was estimated using meteorological data collected at a nearby location. The meteorological data only returned cardinal directions instead of exact angles, giving us an error of $\pm 22.5^\circ$. In addition, wind data were collected every minute, so the wind was chosen closest to the time of each shot. Tables 3 and 4 show, for every shot detected, the distance away from the estimated position to the source using the specified data sets.

Table 3. Source position errors on day 9 using MLE with met data.

	Est. from AOA	Est. from TOA	Est. from Both
Shot	Distance (meters)	Distance (meters)	Distance (meters)
1	26.47	106.32	24.44
2	8.80	96.28	9.90
3	6.29	83.48	6.35
4	22.03	97.47	11.73
5	13.25	88.86	9.17
6	15.71	97.98	7.24
7	31.67	103.11	15.29
8	42.20	112.06	36.70
9	0.72	84.59	8.72
10	34.79	111.27	28.54
11	26.80	110.96	8.36
12	2.01	90.31	7.43
13	32.83	117.53	23.89
14	8.39	36.08	5.07
15	27.08	101.63	25.00
16	48.36	49.27	51.56
17	17.19	121.40	16.90
18	19.20	100.87	9.08
19	41.83	132.95	38.98
20	26.17	118.38	37.02
Median	24.10	101.25	13.51
Mean	22.59	98.04	19.07

Table 4. Source position errors on day 10 using MLE with met data.

	Est. from AOA	Est. from TOA	Est. from Both
Shot	Distance (meters)	Distance (meters)	Distance (meters)
1	15.88	100.41	7.65
2	26.86	104.59	10.88
3	29.83	101.08	4.37
4	14.80	105.59	2.28
5	19.60	134.10	10.96
6	60.46	169.88	50.36
7	38.83	121.56	19.77
8	58.23	114.96	40.87
9	34.31	34.40	24.34
10	32.53	107.69	17.82
Median	31.18	106.64	14.39
Mean	33.13	109.43	18.93

3.3 Estimation Using Blind Wind Compensation

For the blind wind estimation, a maximum likelihood algorithm was employed to find the best estimate. However, to avoid overfitting the data, the blind wind estimation used a single wind speed and direction for all shots to provide a more reasonable and consistent estimate. Using equations 10 and 12, the algorithm searched a 360° circle and selected the best wind direction by

minimizing the error from the estimated AOA and/or TOA. The position and wind direction that minimized the error was selected as the best blind wind estimation. This algorithm was tested for every shot. The direction of the wind was estimated for every shot, and a new source location was also estimated. Tables 5 and 6 show the errors in the source location using the specified data sets. Figures 3 and 4 show the meteorological data collected for every shot and the estimated wind that was chosen.

Table 5. Source estimates' errors with blind wind estimation for day 9.

	Est. from AOA	Est. from TOA	Est. from Both
Shot	Distance (meters)	Distance (meters)	Distance (meters)
1	40.68	106.32	26.36
2	7.39	96.28	9.90
3	8.08	83.48	11.28
4	22.03	97.47	3.59
5	26.02	88.86	9.71
6	26.34	97.98	7.28
7	40.89	103.11	15.29
8	49.99	112.06	33.71
9	8.51	84.59	8.72
10	47.56	111.27	25.68
11	34.61	110.96	9.07
12	13.28	90.31	8.02
13	38.49	117.53	21.56
14	13.38	36.08	4.43
15	41.28	101.63	23.59
16	56.15	49.27	37.05
17	31.92	121.40	9.04
18	30.25	100.87	9.08
19	53.19	132.95	36.17
20	43.16	118.38	25.49
Median	33.26	101.25	10.59
Mean	31.66	98.04	16.75

Table 6. Source estimates' errors with blind wind estimation for day 10.

	Est. from AOA	Est. from TOA	Est. from Both
Shot	Distance (meters)	Distance (meters)	Distance (meters)
1	13.06	100.41	4.59
2	17.79	104.59	9.47
3	23.43	101.08	5.73
4	17.62	105.59	3.66
5	17.44	134.10	3.36
6	61.87	169.88	47.58
7	28.24	121.56	20.53
8	54.70	114.96	38.54
9	33.57	34.40	15.91
10	42.40	105.62	16.05
Median	25.84	105.61	12.69
Mean	31.01	109.22	16.54

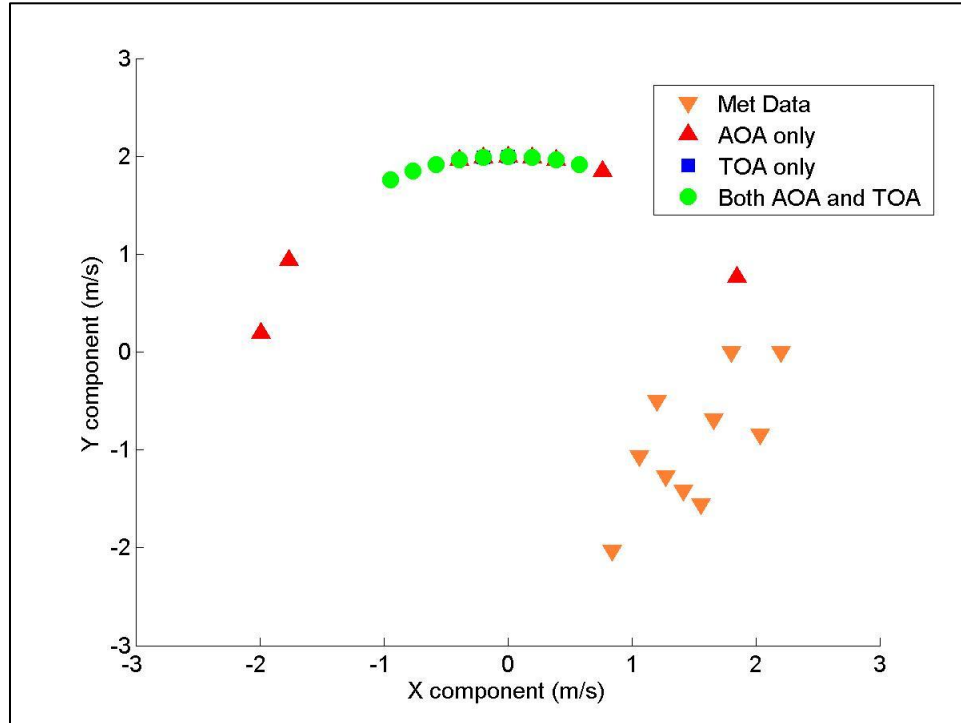


Figure 3. Blind wind estimates day 9.

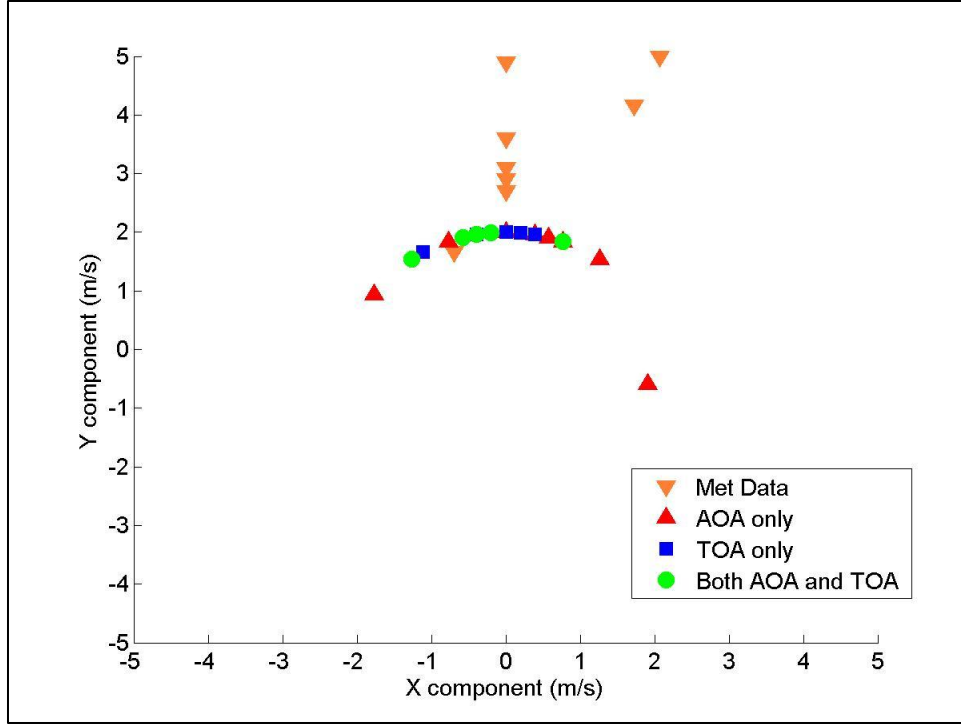


Figure 4. Blind wind estimates day 10.

3.4 Comparative Performance

Wind compensation algorithms affect each shot differently. In addition, any shot may have outliers. Therefore, the mean and standard deviation are not always the best statistic from which to draw conclusions, so median errors are also considered. Tables 7 through 13 show the data metrics (median, mean, and standard deviation) of the errors that were calculated, while figures 5 through 10 are plots of the estimated positions, with the source located at the origin.

Table 7. Results for day 9 without wind compensation.

No wind	Median (meters)			Mean (meters)			Standard Deviation (meters)		
	X	Y	Distance	X	Y	Distance	X	Y	Distance
AOA	-16.94	17.19	22.18	-17.22	18.40	25.32	10.647	11.812	15.705
TOA	-104.86	-21.66	105.82	-82.92	-16.10	103.71	61.004	24.624	22.725
Both	-16.94	17.19	22.18	-17.22	18.40	25.32	10.647	11.812	15.705

Table 8. Results for day 9 with meteorological wind data.

Met Data	Median (meters)			Mean (meters)			Standard Deviation (meters)		
	X	Y	Distance	X	Y	Distance	X	Y	Distance
AOA	-16.83	17.45	24.10	-14.87	15.95	22.59	10.061	11.058	13.679
TOA	-94.86	-31.66	101.25	-72.92	-26.10	98.04	61.004	24.624	22.907
Both	-10.79	7.19	13.51	-12.12	8.80	19.07	13.837	11.736	13.518

Table 9. Results for day 9 with blind wind estimation.

Blind	Median (meters)			Mean (meters)			Standard Deviation (meters)		
	X	Y	Distance	X	Y	Distance	X	Y	Distance
AOA	-24.25	23.75	33.26	-21.17	23.40	31.66	10.579	11.706	15.570
TOA	-94.86	-31.66	101.25	-72.92	-26.10	98.04	61.004	24.624	22.907
Both	-8.75	7.69	10.59	-8.87	8.55	16.75	10.815	11.715	10.898

Table 10. Results for day 10 without wind compensation.

No wind	Median (meters)			Mean (meters)			Standard Deviation (meters)		
	X	Y	Distance	X	Y	Distance	X	Y	Distance
AOA	-17.33	17.39	25.53	-20.20	21.16	29.33	10.319	11.937	15.628
TOA	-98.94	-31.17	110.82	-85.26	-0.52	116.59	54.851	70.612	35.372
Both	-12.03	13.22	17.87	-15.39	15.29	22.36	12.941	13.676	17.971

Table 11. Results for day 10 using meteorological wind data.

Met Data	Median (meters)			Mean (meters)			Standard Deviation (meters)		
	X	Y	Distance	X	Y	Distance	X	Y	Distance
AOA	-18.42	17.65	26.86	-20.41	21.43	29.65	9.591	10.219	13.894
TOA	-94.81	-41.99	105.59	-77.01	-14.03	109.34	55.151	63.181	28.108
Both	-10.25	3.65	10.88	-11.01	7.43	14.19	11.556	10.259	14.566

Table 12. Data error metrics for day 10 with blind wind estimation.

Blind	Median (meters)			Mean (meters)			Standard Deviation (meters)		
	X	Y	Distance	X	Y	Distance	X	Y	Distance
AOA	-18.12	18.37	25.84	-21.71	22.05	31.01	11.618	12.475	16.916
TOA	-94.53	-40.95	105.61	-69.01	-14.95	109.22	64.928	68.118	33.787
Both	-10.10	6.21	12.69	-12.01	10.15	16.54	11.277	11.694	15.324

Table 13. Percent reduction in distance error over no wind estimate.

	Median		Mean		Standard Deviation	
	Met	Blind	Met	Blind	Met	Blind
Day 9	39.1%	52.2%	24.7%	33.9%	13.9%	30.6%
Day 10	47.0%	29.0%	35.6%	26.0%	20.1%	14.7%

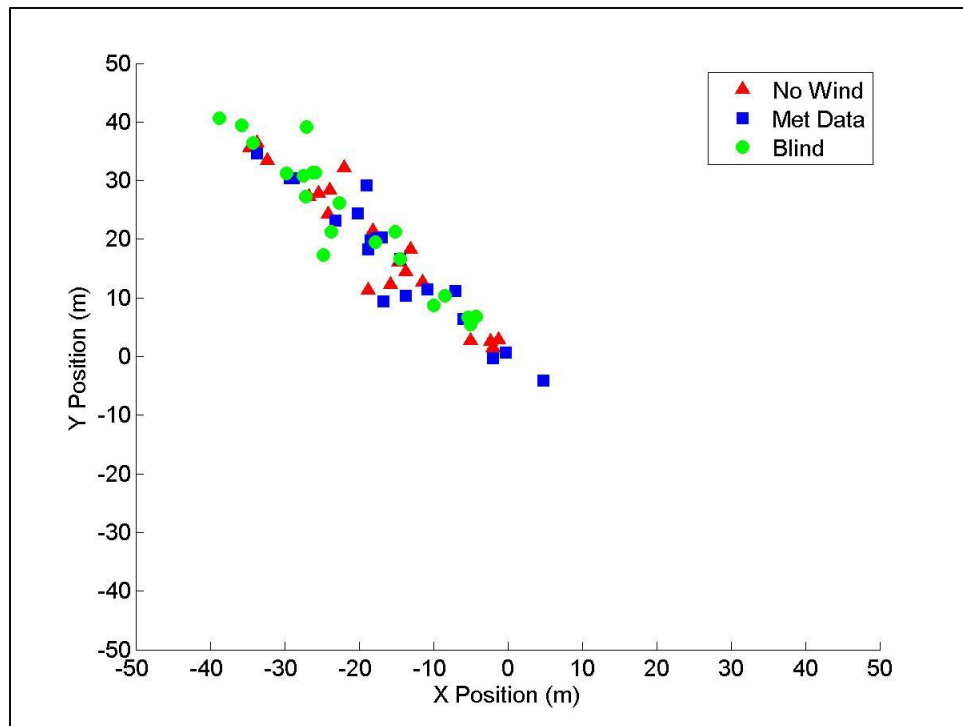


Figure 5. Estimated position error using AOA data only on day 9.

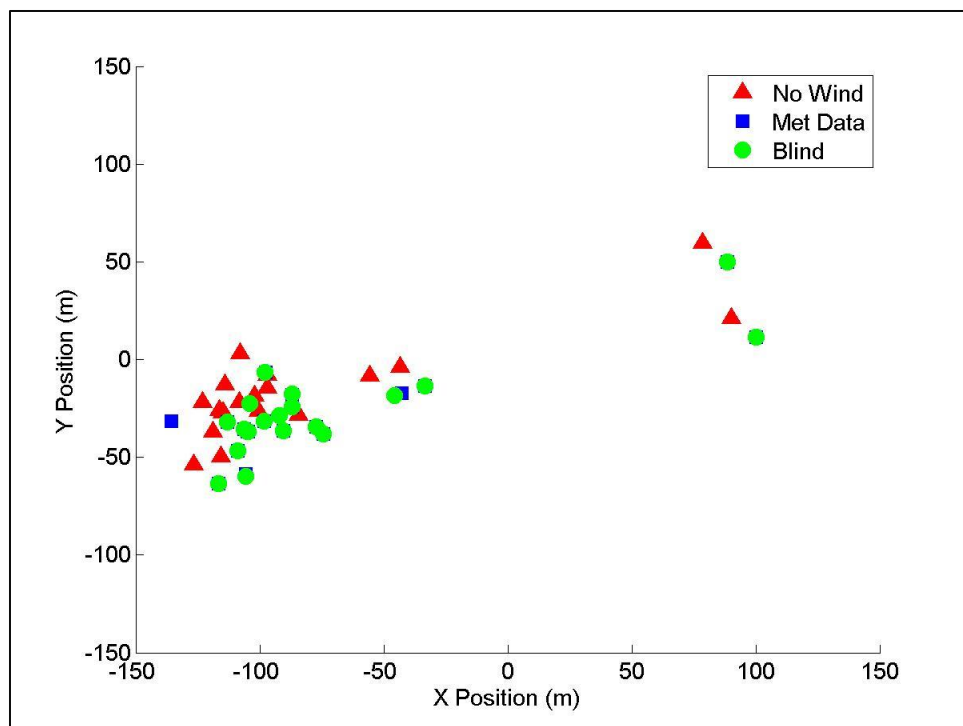


Figure 6. Estimated position error using TOA data only on day 9.

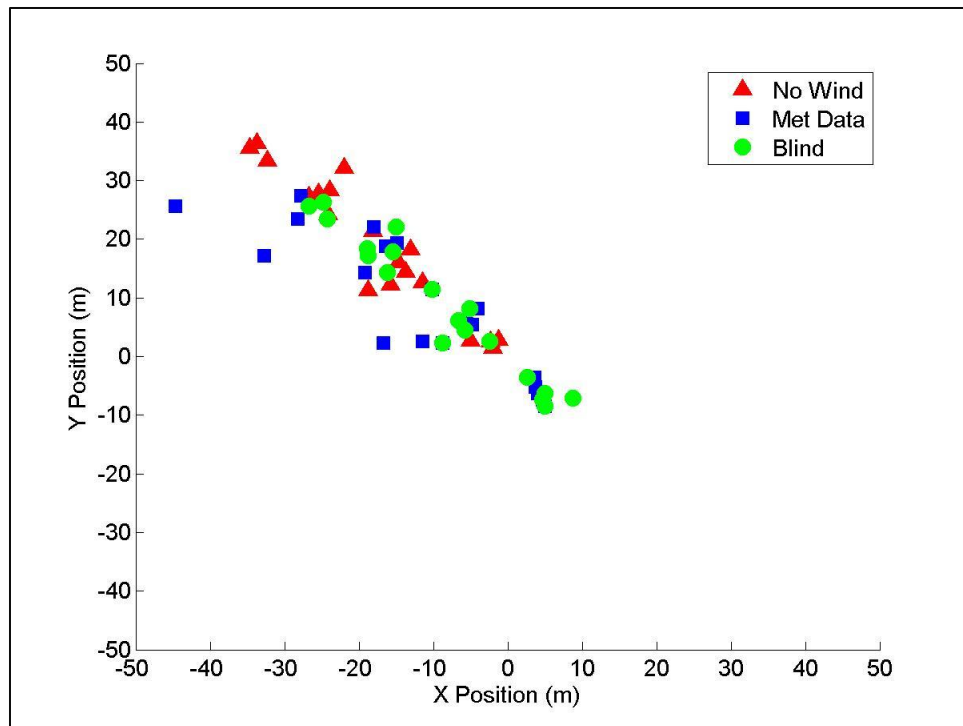


Figure 7. Estimated position error using both AOA and TOA data on day 9.

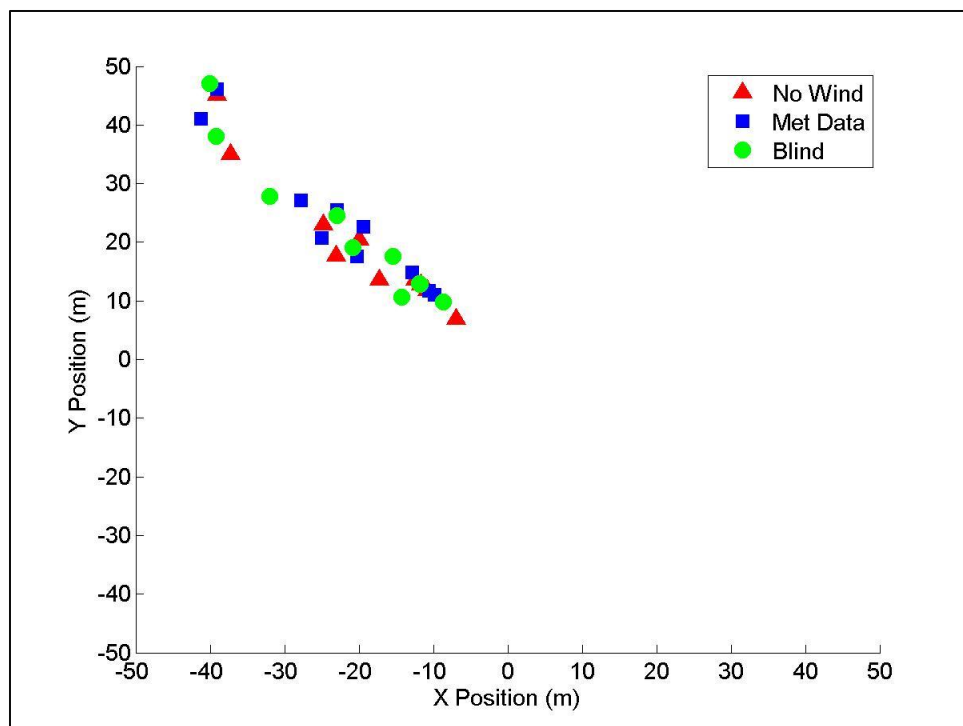


Figure 8. Estimated position error using AOA data only on day 10.

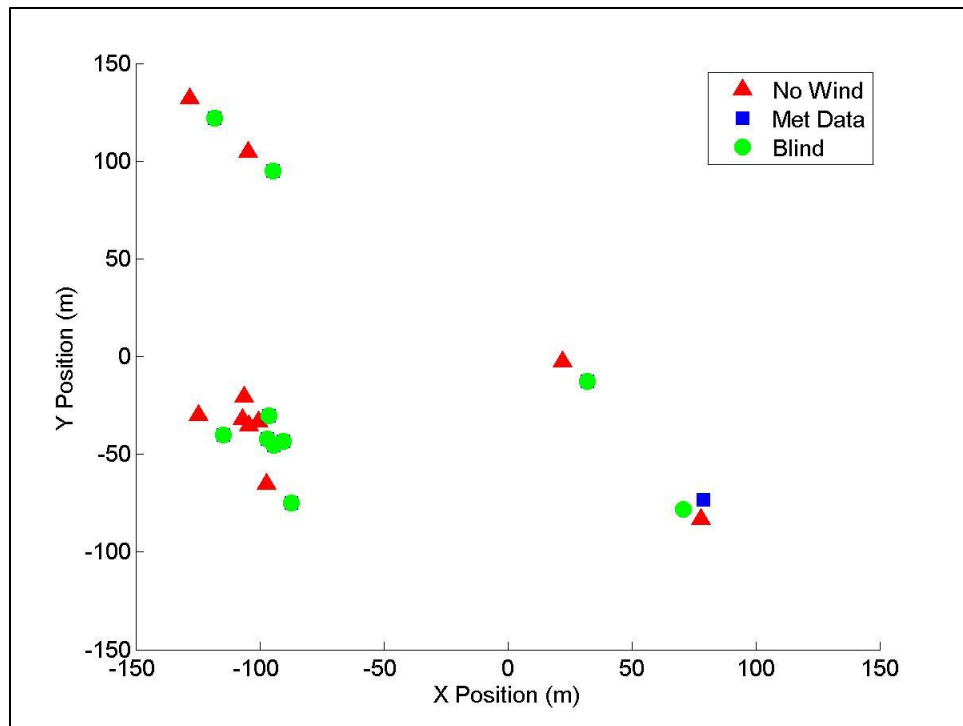


Figure 9. Estimated position error using TOA data only on day 10

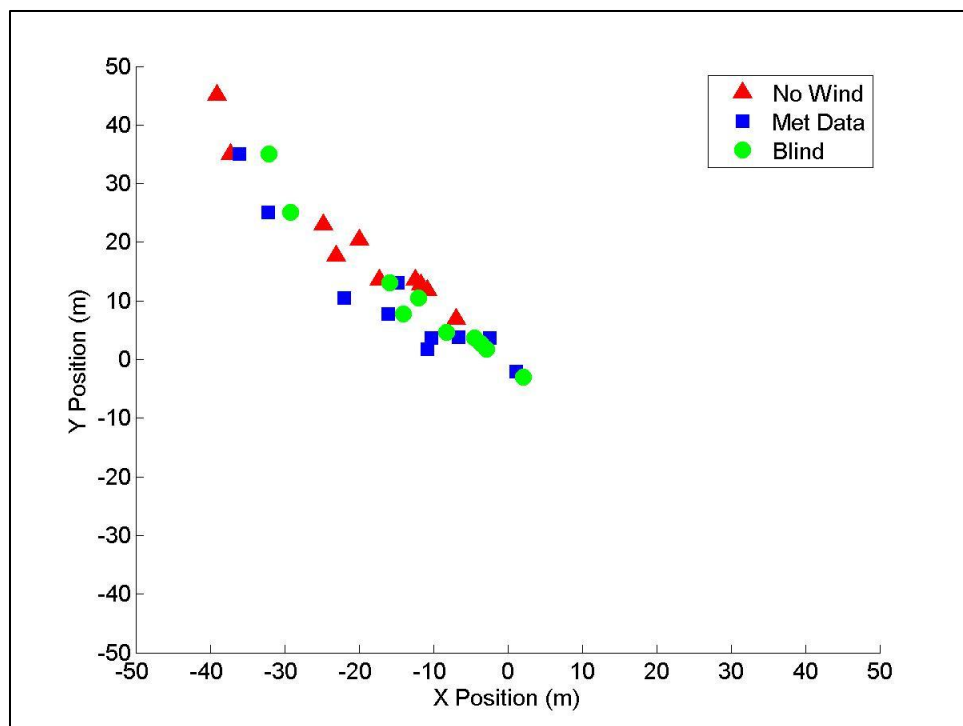


Figure 10. Estimated position error using both AOA and TOA data on day 10

While the data suggest that the blind wind estimation improves the source estimates fairly well, the blind wind estimates do not match the measured wind direction data. According to figure 3, on day 9, the wind direction selected varied greatly from east and west, and consistently pointed north instead of the south as the meteorological data reported. On day 10, figure 4 indicates the blind wind estimation performed slightly better, choosing values that consistently pointed north, thus agreeing with the meteorological data, but varied east and west. However, differing wind speeds and directions at the arrays and the meteorological data collector may explain this.

In figures 5 and 8, only the AOA data were used, and wind compensation made only minor improvements on localizing the source. While the accuracy of the estimate worsened slightly, the standard deviation reduced, thus improving the consistency of the results with wind compensation (as seen with the tighter cluster of estimates with wind compensation). Nonetheless, using both TOA and AOA improves accuracy and consistency better than using AOA alone, so using only AOA data is not the best choice.

In figures 6 and 9, only the TOA data were used, and they performed poorly. Prior to wind compensation, the localization errors using only TOA data were inaccurate and the wind compensation algorithms, whether blind or using meteorological data, only slightly improved the results. This error is consistently greater than estimates using AOA data, often three to four times larger according to tables 7 through 12. It can be explained by the inability to use TOA data from Array 4, the saturated array. Without this data set, the algorithm loses sensitivity, which can cause large overshoots. Array 4 is critical because it is located a large distance away to the southwest from the other arrays, giving information concerning north and south localization. This is confirmed when both data sets are used.

Figures 7 and 10 used both TOA and AOA data, and those estimates are not primarily located south from the true position and more closely resembles the estimates from the AOA data. The best and most reliable estimated positions are found using the meteorological data with both TOA and AOA data sets. This was expected since that method used the actual wind data, in addition to all the processed data available. Observing the median and mean distance errors, the results indicate a significant improvement. Table 13 shows percent reduction in error when comparing the distance error between the no wind estimates and the wind compensated estimates. Though tables 7, 9, 10, and 12 indicate the standard deviation increases in the x-direction considerably on day 9, the normalized standard deviation on both days improves significantly, thus overall the variance of the results decreases making it the more reliable result.

Using blind wind compensation revealed interesting and unexpected results. Although day 9's wind estimates for blind wind compensation was consistently incorrect, the results show a better mean and median improvement in source estimates over using meteorological data. Despite this, blind wind compensation is not recommended as the better method because the wind velocity estimates are inconsistent with the meteorological data. One reason for this may stem from the inability to use TOA data from Array 4 to provide some sensitivity to the north and south. In

addition, day 10 experienced higher wind speeds and varied more than day 9 in terms of wind speed. Overall, both days suffered because of the saturated array and errors within the array hardware and software. User-defined TOA and AOA data in simulations revealed the blind wind estimation algorithms returned good wind estimates, both in speed and direction, even when error was introduced to the data.

Despite one degree of freedom being removed, the blind wind estimation still pointed in varying directions, often 90° or more off what the meteorological data asserts, as seen in figure 3.

Interestingly, in figure 4, despite its higher variance in true wind speed, day 10 returned wind estimate directions that more closely resembled the true wind direction, yet performed worse in source localization when using blind wind estimation over using meteorological data.

Meanwhile, day 9 returned wind directions that disagreed with the meteorological data, yet performed better in source localization when using blind wind estimation.

4. Conclusions

Techniques for source localization and wind compensation with acoustic signals were developed and tested. TOA and AOA were computed at each array then processed using least squares and maximum likelihood approaches.

Estimates of the position of the source were spread, but improvements were made after including wind compensation. The localization errors may be caused by the time offsets between the previously processed TOA estimates and the new TOA estimates calculated. Using both TOA and AOA in localization and wind compensation, improvements were found in median, mean, and standard deviation of the errors. Wind compensation always improves results.

Meteorological data provide the most improved results. Blind wind compensation still showed some improvements in accuracy and reduced variance compared to the no wind estimates, and at times, performed better than the meteorological data, despite not finding the correct wind. Blind wind compensation algorithm is not recommended, despite its good localization results.

5. References

1. Scanlon, M.; Reiff, C.; Solomon, L. Aerostat Acoustic Payload for Transient and Helicopter Detection. *Proc. SPIE* 6538, 2007.
2. Pham, T.; Sadler, B. M. Wideband Array Processing Algorithms for Acoustic Tracking of Ground Vehicles. *Proc. 21th Army Science Conference*, 1998.
3. Naz, P.; Marty, C.; Hengy, S.; Miller, L. S. Acoustic Detection and Localization of Weapons Fire via Unattended Ground Sensors and Aerostat-borne Sensors. *SPIE*, 2009
4. Goldman, G.; Reiff, C. Localization Using Ground- and Air-based Acoustic Arrays. *SPIE*, 2011.
5. Kaplan, L. M.; Le, Q. On Exploiting Propagation Delays for Passive Target Localization Using Bearings-only Measurements. *Journal of the Franklin Institute* **March 2005**, 324 (2), 193–211.
6. Yao, K.; Chen, J.; Hudson, R. Maximum-Likelihood Acoustic Source Localization: Experimental Results. *IEEE*, University of California, Los Angeles, 2002.
7. Goldman, G.; Duong, T. *Effect of Microphone Calibration on Localization of Transient Signals*, Dec. 2008.
8. Papoulis, A.; Pillai, S. *Probability, Random Variables, and Stochastic Processes*; McGraw-Hill, 2002.

List of Symbols, Abbreviations, and Acronyms

AOA	angle of arrival
BPRF	Blossom Point Research Facility
DOA	direction of arrival
DTOA	differential time of arrival
GPS	global positioning system
HEDG	Heading
LOBR	Line of Bearing
MLE	maximum likelihood estimate
TOA	time of arrival

NO. OF COPIES	ORGANIZATION
1 ELEC	ADMNSTR DEFNS TECHL INFO CTR ATTN DTIC OCP 8725 JOHN J KINGMAN RD STE 0944 FT BELVOIR VA 22060-6218
4	US ARMY ARDEC FUZE PRECISION ARMAMENT TECHNOLOGY DIV ATTN A MORCOS ATTN H VANPELT ATTN J CHANG ATTN S DESAI BLDG 407 PICATINNY ARSENAL NJ 07806
6	US ARMY RSRCH LAB ATTN IMAL HRA MAIL & RECORDS MGMT ATTN RDRL CIO LL TECHL LIB ATTN RDRL SES P G GOLDMAN ATTN RDRL SES P M SCANLON ATTN RDRL SES S G WILLIAMS ATTN RDRL SES S R HOLBEN ADELPHI MD 20783-1197